

PARAMETERIZATION OF THE COLLECTION EFFICIENCY CURVE OF CATCHING-TYPE GAUGES BASED ON RAINFALL INTENSITY

Arianna Cauteruccio^{1,2*} & Luca G. Lanza^{1,2}

(1) Department of Civil, Chemical and Environmental Engineering, University of Genova, Genova, Italy

(2) WMO/CIMO Lead Centre "B. Castelli" on Precipitation Intensity, Italy

*email: luca.lanza@unige.it

KEY POINTS

- Wind is the main environmental source which affects precipitation measurements.
- Numerical simulations allow to derive adjustment curves as a function of wind speed.
- An adjustment curve for a cylindrical gauge and for the Italian territory is derived.
- The adjustment curve is parameterized with the rainfall intensity.

1 INTRODUCTION

In operational practice, adjustment curves to account for wind-induced biases of precipitation measurements are rarely adopted, due to the complexity of their formulation. The effect of wind was indeed studied in the literature using different approaches (field measurement campaigns, numerical simulation and wind tunnel experiments) with the aim of formulating correction curves to calculate the actual precipitation falling to the ground. In field tests, the ratio between the precipitation measured by a gauge in operational conditions and a reference one provides the Collection Efficiency (CE) for any given wind speed. The numerical approach, based on Computational Fluid Dynamic (CFD) simulations of the airflow field and the modelling of hydrometeors trajectories, which can be validated in wind-tunnel tests, allows to investigate different configurations by varying the wind speed, type of precipitation and gauge geometry.

The analysis of field data allowed to formulate various correction curves, most of them focused on solid precipitation, usually obtained as a function of wind speed and air temperature (e.g. *Førland et al.*, 1996; *Wolff et al.*, 2015 and *Buisán et al.*, 2017). CE curves that are derived from field experiments alone, depend on the site where the test field is located, its precipitation and wind climatology, and a large dispersion of the field measured data around the best-fit curves usually persists. Based on the dependence of such curves on the drop size distribution, and given its link with the precipitation intensity, *Colli et al.* (2019) recently showed that such dispersion can be reduced by including the results of the numerical simulation into the best-fit methodology. The authors analyzed quality controlled snowfall data from the Marshall field-test site (CO, USA) and revealed that the wind-induced undercatch of solid precipitation gauges is best correlated with the measured snowfall intensity, rather than temperature, in addition to wind speed. This dependency from the precipitation intensity was previously shown by *Førland et al.* (1996) in case of liquid precipitation.

In the present work, an easy to use Collection Efficiency formulation, is obtained as a function of wind speed and rainfall intensity for a typical cylindrical catching-type gauge by using numerical simulation results. The airflow fields (velocity magnitude and components) around the Casella[®] tipping-bucket gauge, obtained from numerical simulations at various wind speeds and partially published in the work of *Colli et al.* (2018), were adopted. Starting from these simulations the use of the Lagrangian Particle Tracking (LPT) model adopted by *Colli et al.* (2015) for solid precipitation and here modified by introducing a drag coefficient formulation suitable for liquid particles, allowed to obtain the catch ratios for drops of various size. Then the collection efficiency was calculated from Equation 1 as the integral over the whole range of diameters after the introduction of a suitable Particle Size Distribution (PSD) based on data from the Italian territory (*Caracciolo et al.* 2008) and fitted by using the typical exponential function (Marshall-Palmer distribution, from *Marshall & Palmer*, 1948). In Equation 1, ρ_p and V_p are the density and volume of the rain drops modelled with spherical shape, $n_{max}(d)$ and $n(d)$ are the number of particles for each diameter, which should fall inside the gauge collector if the airflow field was not affected by the aerodynamic response of the gauge body and that are collected in disturbed conditions, while $N(d)$ is the total number of particles per unit volume of air and per unit size interval having volume equal to the sphere of diameter d .

$$CE(U_{ref}) = \frac{\int_0^d \rho_p V_p n(d) N(d) dd}{\int_0^d \rho_p V_p n_{max}(d) N(d) dd} \quad (1)$$

2 METHODOLOGY

Reynold Average Navier-Stokes (RANS) simulations conducted for various wind speeds U_{ref} equal to 2-5-7-10-18 m s⁻¹ around a Casella[®] tipping-bucket cylindrical gauge, were adopted in the LPT model to calculate the catch ratios for drops with equivalent diameter d equal to 0.25 - 0.5 - 0.75 mm and from 1 to 8 mm, with a bin size of 1mm. In order to obtain a single CE curve, as a function of wind speed and rainfall intensity in the respective investigated ranges, three steps were followed, as summarized below:

- A Marshall-Palmer (MP) distribution was fitted to the particle size measured data provided by *Caracciolo et al.* (2008) and the associated parameters N_0 and Λ , per each RI class, were adopted in Equation 1 to calculate the raw CE values. A four parameter sigmoidal function was fitted to these values to obtain the CE curves as a function of wind speed, per each RI class.
- The variation of the N_0 and Λ parameters obtained in a), attributed to the mean value of each RI class, was interpreted by power law curves as a function of RI, and new sigmoidal curves were obtained for the CE calculated from the fitted parameters. Interpreting N_0 and Λ as a function of RI allows obtaining the MP parameters for any RI value within the investigated range.
- Finally, with the objective to obtain a simple formulation for the CE as a function of both RI and U_{ref} in the investigated ranges, also the variation of the four parameters of the sigmoidal function was interpreted as a function of RI, using either power laws or logarithmic functions.

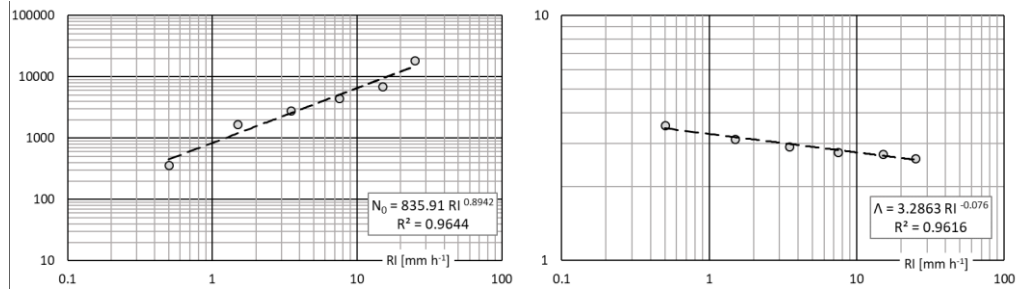


Figure 1. MP parameters (N_0 on the left and Λ on the right) associated with the mean values of each RI class (circles) and fitted by power law curves (dashed lines).

3 RESULTS AND DISCUSSION

The procedure is applied below to real-world observations. The average observed PSD measured by the Pludix disdrometer in the Florence experimental site as provided by *Caracciolo et al.* (2008), classified for six rainfall intensity categories, were fitted using the typical MP exponential function. The parameters N_0 [mm⁻¹ m⁻³] and Λ [mm h⁻¹], and the correlation factors (R^2) for each RI class are listed in Table 1. For all RI classes, R^2 is larger than 0.97, indicating a good fit between observations and the MP curves. Furthermore, as expected, Λ decreases, while N_0 increases, with increasing RI because heavy rainfall events are characterized by a relatively higher number of drops of large diameter in the distribution and by an overall higher number of particles in one cubic meter of air.

Following step a), for each simulated wind speed, the raw CE values were numerically calculated, by using for the PSD the best-fit MP parameters associated with each RI class (from Table 1) and interpolated with a four parameters sigmoidal curve (Eq. 2), and the obtained parameters' values are listed in Table 2. Following step b), with the aim to make explicit the dependence of CE on rainfall intensity, N_0 and Λ were assigned to the mean value of each RI class and interpolated with power law curves as shown in Figure 1.

RI class [mmh ⁻¹]	R≤1	1≤R<2	2≤R<5	5≤R<10	10≤R<20	R>20
N ₀ [mmh ⁻¹ m ⁻³]	365.1	1692.8	2775	4459	6989.4	18370
Λ [mmh ⁻¹]	3.561	3.134	2.914	2.771	2.723	2.609
R ²	0.979	0.976	0.979	0.975	0.972	0.979

Table 1. Parameters N₀ and Λ of the MP distribution and R² for each rainfall intensity class, obtained by fitting the PSD provided by Caracciolo et al. (2008).

$$CE(U_{ref}) = y_0 + \frac{a}{1 + e^{-\frac{(U_{ref}-x_0)}{b}}} \quad (2)$$

RI class [mmh ⁻¹]	R≤1	1≤R<2	2≤R<5	5≤R<10	10≤R<20	R>20
a	0.2632	-0.1995	0.1696	0.1513	0.1454	0.1317
b	-4.2495	4.067	-3.9526	-3.871	-3.8422	-3.7713
x ₀	3.8429	4.7512	5.251	5.5914	5.709	5.996
y ₀	0.8445	1.0753	0.892	0.9024	0.9058	0.914
R ²	0.984	0.984	0.983	0.982	0.982	0.982

Table 2. Parameters of the sigmoidal functions obtained by fitting the raw CE values derived by using the MP parameters from the exponential interpolations and correlation factors for each RI class.

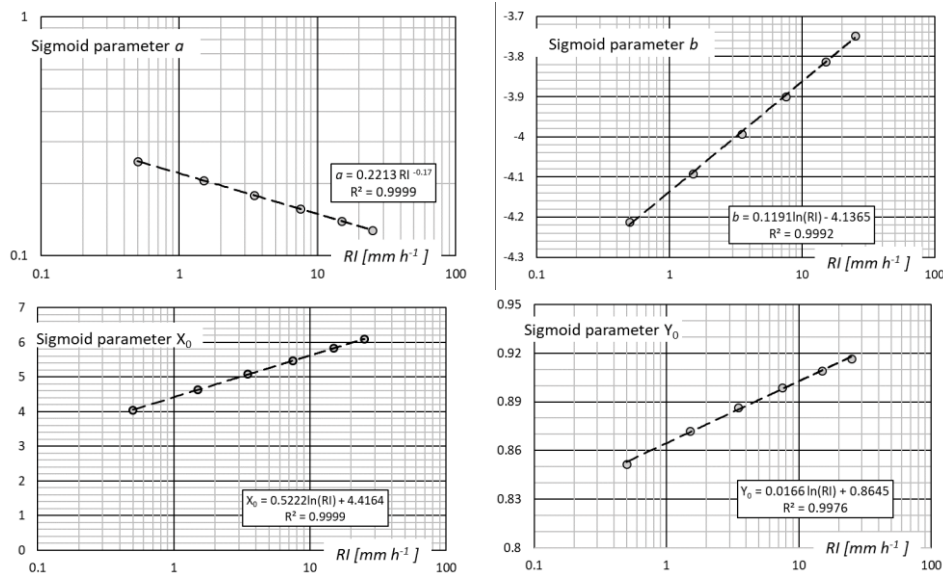


Figure 2. Sigmoidal parameters (*a* and *b* in the upper panels, *X*₀ and *Y*₀ in the bottom panels), associated with the mean value of each RI class (circles) and fitted by either power law or logarithmic curves (dashed lines).

	R≤1 [mmh ⁻¹]	1≤R<2 [mmh ⁻¹]	2≤R<5 [mmh ⁻¹]	5≤R<10 [mmh ⁻¹]	10≤R<20 [mmh ⁻¹]	R>20 [mmh ⁻¹]
a	0.2481	0.2069	0.1794	0.1574	0.1395	0.1275
b	-2.127	-4.0923	-3.9925	-3.8994	-3.8128	-7.481
x ₀	4.043	4.6353	5.0803	5.4739	5.8284	6.0888
y ₀	0.8516	0.872	0.8866	0.8988	0.9093	0.9165
R ²	0.984	0.984	0.983	0.983	0.982	0.981

Table 3. Parameters of the sigmoidal functions obtained by using N₀(RI) and Λ(RI) expressed by the power law curves and R².

Then, the N₀ and Λ values provided by the power law curves (Figure 1, dashed lines) were adopted to calculate the new CE values, and the parameters for the sigmoidal functions as listed in Table 3. The obtained CE curves are depicted in Figure 2 (left-hand panel dashed lines) and compared with the raw CE values (diamond) calculated under step a). This further step provides an important advantage because it

allows to derive the PSD for any desired rainfall intensity within the measured RI range ($0.5\text{--}25\text{ mm h}^{-1}$).

Finally, as summarized in step c), a general formulation for the CE (Eq. 2) as a function of both RI and U_{ref} , but independent on the initial RI classes and valid throughout the investigated RI range, was obtained by fitting the sigmoidal parameters associated with the mean value of each RI class with logarithmic (for b , x_0 , y_0) and power law (for the parameter a) curves (see Figure 2). The general expression is as follows:

$$CE(U_{ref}) = y_0(RI) + \frac{a(RI)}{1 + e^{-\frac{(U_{ref}-x_0(RI))}{b(RI)}}} \quad (2)$$

Finally, the collection efficiency curves were calculated by using Eq. 2 for the mean value of each RI class (Figure 2 left-hand panel continuous lines) as already done in steps a) and b). Then, the correlation between the raw CE values and the curves obtained in the three steps (a), b) and c)) were compared as shown in Figure 2 for each RI class. This result shows in all cases very high values of the correlation factor, larger than 0.99, and for step a) is only slightly higher than step c) (about $+10^{-5}$). This very minimal worsening of performance is counterbalanced by the simplification introduced by the final CE curve, which allows to easily apply a correction factor for the wind induced-error of operational precipitation measurements.

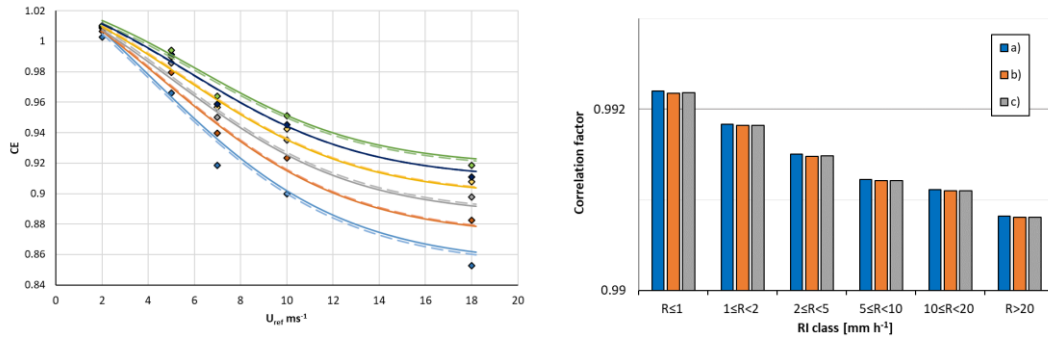


Figure 2. Left-hand panel: raw CE values (diamonds) obtained by using the MP parameters derived from the exponential interpolation (step a)), for each RI class. CE curves obtained by expressing N_0 and Λ as a function of RI (dashed lines, step b)) and by expressing the sigmoidal parameters as a function of RI (continuous lines, step c)). Right-hand panel: correlation factors between the raw CE values and the CE curves obtained, for each RI class, under step a) (blue), b) (orange) and c) (grey).

REFERENCES

- Buisán, S.T., Earle, M.E., Collado, J.L., Kochendorfer, J., Alastrué, J., Wolff, M., Smith, C.D. & López-Moreno, J.I. Assessment of snowfall accumulation underestimation by tipping bucket gauges in the Spanish operational network, *Atmospheric Measurements Techniques*, 2017, 10, 1079–1091.
- Caracciolo, C., Porcù, F. & Prodi, F. Precipitation classification at mid-latitudes in terms of drop size distribution parameter. *Advances in Geosciences*, 2008, 16, 11–17.
- Colli, M., Lanza, L.G., Rasmussen, R., Thériault, J.M., Baker, B.C. & Kochendorfer, J. An improved trajectory model to evaluate the collection performance of snow gauges. *Journal of Applied Meteorology and Climatology*, 2015, 54, 1826–1836.
- Colli, M., Pollock, M., Stagnaro, M., Lanza, L.G., Dutton, M. & O’Connell, P.E. A Computational Fluid-Dynamics assessment of the improved performance of aerodynamic raingauges. *Water Resource Research*, 2018, 54, 779–796.
- Colli, M., Stagnaro, M., Thériault, J.M., Lanza, L.G. & Rasmussen, R. Adjustments for Wind-Induced Undercatch in Snowfall Measurements based on Precipitation Intensity. *Journal of Hydrometeorology*, 2019, (accepted).
- Førland, E. J., Allerup, P., Dahlström, B., Elomaa, E., Jónsson, T., Madsen, H., Perälä, J., Rissanen, P., Vedin, H. & Vejen, F. Manual for operational correction of Nordic precipitation data, DNMI report Nr. 24/96, Norwegian Meteorological Institute, Oslo, Norway, 1996.
- Marshall, J.S. & Palmer, W.M.K. The distribution of raindrops with size. *Journal of Meteorology*, 1948, 5, 165–166.
- Wolff, M. A., Isaksen, K., Petersen-Øverleir, A., Ødemark, K., Reitan, T. & Brækkan, R. Derivation of a new continuous adjustment function for correcting wind-induced loss of solid precipitation: results of a Norwegian field study, *Hydrology and Earth System Sciences*, 2015, 19, 951–967.

Acknowledgements

This work was developed in the framework of the Italian national project PRIN20154WX5NA “Reconciling precipitation with runoff: the role of understated measurement biases in the modelling of hydrological processes”.